On the Interaction between the Gulf Stream and the New England Seamount Chain

TAL EZER

Program in Atmospheric and Oceanic Sciences, Princeton University, Princeton, New Jersey

22 June 1992 and 9 March 1993

ABSTRACT

In the course of numerical simulations with a primitive equation regional model of the Gulf Stream, bottom topography and the New England Seamount Chain (NESC) in particular show significant influence on the variability and the energetics of the Gulf Stream system. The model is an eddy-resolving, coastal ocean model that includes thermohaline dynamics and a second-order turbulence closure scheme to provide vertical mixing coefficients; it is driven at the surface by observed monthly wind stress and heat fluxes. The surface and the deep variabilities obtained from the numerical simulations are in fair agreement with the observed variabilities inferred, for example, from the Geosat altimetry data and from measurements of eddy kinetic energy (EKE).

To study how the NESC affects the Gulf Stream dynamics, a control run without the NESC (however, leaving the other topographic features such as the continental shelf and slope intact) is compared to simulation with full bottom topography. According to the model results, the effects of the NESC on the Gulf Stream include southward deflection of the stream as it passes across the NESC and the development of several quasi-stationary, nearly barotropic recirculation cells on both sides of the Gulf Stream. Another result is an *increase* in the mean kinetic energy (MKE) and a *decrease* in the EKE in most of the water column as a result of the inclusion of the NESC. The inclusion of the NESC causes an upstream shift in the area of maximum variability compared with the case without the NESC; the maximum deep EKE is thus obtained upstream of the NESC. This study suggests that the stabilizing effects of the bottom topography dominate over possible destabilizing effects due to increase in meander amplitudes near the NESC. This study also suggests that the NESC causes a downstream decrease in the propagation speed of meanders upstream of the NESC and the development of an almost steady, large meander downstream of the NESC.

1. Introduction

The importance of topographic effects on ocean circulation has been demonstrated for a long time; several observational and numerical studies have been focused for example, on the interaction between western boundary currents and the bottom topography. Of particular interest in the western North Atlantic is the possible influence that the New England Seamount Chain (NESC) may have on the Gulf Stream dynamics. The NESC consists of a series of seamounts with different sizes and heights; they have a diameter comparable to the Rossby radius of deformation of the ocean in this region, and some of them rise to more than half the ocean depth.

Analysis of fluctuating flows in the deep western North Atlantic suggests that bottom friction may balance all the energy input by the wind and that most of this dissipation occurs in a small region near the NESC (Weatherly 1984). Interaction between the NESC and the Gulf Stream is thus expected; however, there is conflicting evidence of the exact way in which the NESC affects the Gulf Stream path and variability [Cornillon (1986) reviews some of these observations]. For example, while some observations suggest a dramatic increase of Gulf Stream meander amplitudes and envelop downstream of the NESC (e.g., Richardson 1983; Teague and Hallock 1990), satellite infrared images analyzed by Cornillon (1986) show that downstream of the NESC, the Gulf Stream envelope is nearly the same as over the seamounts and that the downstream rate of increase of meander amplitudes is similar to the rate upstream of the NESC. Inverted echo sounders and Geosat altimeter crossover data used by Hallock et al. (1989) did not show significant differences between the regions upstream and downstream of the NESC, in contrast to a more recent study using model and observations (Hallock et al. 1991). A five-year climatological survey conducted by Auer (1987) indicates that the NESC region has the largest frequency of warm-core eddy formations. These and other observations strongly suggest that there are some interesting changes in the dynamics of the Gulf Stream as it transits the NESC. However, one cannot be certain that the NESC is the sole factor responsible for these changes. For example, an area of maximum heat flux and wind stress are found around the location of the NESC, so local atmospheric forcing may also be responsible for changes in the Gulf Stream there [e.g.,

Corresponding author address: Dr. Tal Ezer, Atmospheric and Oceanic Sciences, Princeton University, Sayre Hall, P.O. Box CN710, Princeton, NJ 08544-0710.

Ezer and Mellor (1992) show the atmospheric forcing for the western North Atlantic, as obtained from the Oberhuber (1988) atlas].

Since oceanic observations are usually too sparse in space and time to describe the three-dimensional mesoscale dynamics of the ocean, high-resolution numerical ocean models are being used to study different processes on such scales. Recently, basin-scale numerical models became realistic enough to resolve mesoscale topographic features as well as mesoscale oceanic processes. The Community Modeling Effort (CME) of the World Ocean Circulation Experiment (WOCE) provides, for example, an eddy-resolving basin-scale model for the North Atlantic Ocean (Bryan and Holland 1989; Treguier 1992). However, the Gulf Stream region is still not well resolved by this basin-scale model, and the stream tends to overshoot the observed separation point; this pathological behavior of numerical models has been studied by Thompson and Schmitz (1989), who used a two-layer regional primitive equation model and showed that the deep western boundary current (DWBC) plays an important role in the Gulf Stream separation problem. The recent study of Ezer and Mellor (1992), using a regional coastal ocean primitive equation model, shows that a realistic Gulf Stream separation is obtained when realistic atmospheric forcing is used and when the observed slope water inflow along the continental slope (from the northeast) is specified. Because regional models of this type are largely controlled by the flows specified on the open boundaries, the separation problem is now being studied with basin-scale models.

Numerical models can be used to test the hypothesis that the NESC is responsible for changes in the Gulf Stream, by calculating a control case in which bottom topography is neglected (i.e., a flat bottom case). Experiments of this type have been done before; they show, for example, that southward deflection of the stream (Adamec 1988) and large change in the eddy kinetic energy field (Thompson and Schmitz 1989) may be attributed to the interaction of the stream with the NESC. However, these studies used relatively simple models (quasigeostrophic dynamics with a square domain in the former study, and a two-layer primitive equation layered model in the latter one). The above experiments strongly suggest the need for more realistic models with better vertical resolution; for example, significant changes in the interaction of a midlatitude jet with bottom topography were found by Adamec (1988) between simulations with one baroclinic mode and simulations with two.

Here, we use a more realistic model than those used in previous studies: the Princeton ocean model of Blumberg and Mellor (1987), which includes the continental shelf and slope and is forced by observed monthly heat flux and wind stress. In its Gulf Stream version, it has better resolution and larger domain than the previous studies of Mellor and Ezer (1991) and Ezer and Mellor (1992).

The numerical ocean model is described briefly in section 2. The numerical experiments are presented and the results are discussed in sections 3 and 4. Conclusions are offered in section 5.

2. The ocean model

The numerical ocean model used here is described in detail by Blumberg and Mellor (1987); it is a three-dimensional, free surface, coastal ocean model with a second-order turbulence closure scheme (Mellor and Yamada 1982) to provide vertical mixing coefficients. The model has been used, for example, to study bays and estuaries and many coastal regions around the world. In the Gulf Stream region it has been used in a smaller domain to test altimetry data assimilation schemes (Mellor and Ezer 1991), to study the interaction between the deep and the coastal ocean (Oey et al. 1992), and to study the effects of atmospheric forcing on Gulf Stream separation (Ezer and Mellor 1992). The model with the extended domain used here, has been used to evaluate the forecast skill of the model (Ezer et al. 1992) and to compare sea surface height derived from diagnostic calculation with Geosat altimetry data (Ezer et al. 1993).

The vertical grid uses a sigma coordinate system (i.e., bottom-following vertical grid) with 15 layers; the horizontal grid uses a coastal-following, curvilinear orthogonal grid system. The horizontal grid used here is shown in Fig. 1a, the bottom topography used in the experiments described later are shown in Figs. 1b,c. The horizontal resolution in the Gulf Stream region is now $\sim$10–17 km compared to 20–25 km in the previous studies of Mellor and Ezer (1991) and Ezer and Mellor (1992); the model domain is also larger than that used in those studies. The prognostic variables of the model are the free surface η, potential temperature T, salinity S (hence density ρ), and velocity (U, V, W). The numerical scheme has a split time step, an external mode that solves the vertically integrated momentum equation, and an internal mode that solves the three-dimensional momentum, heat, and salt equations. Further details of the numerical techniques are given in the papers mentioned above.

Since it is a regional model, open boundary conditions either are specified according to observations or have a radiation condition. Near the southwest corner of the model, at the Florida Straits, a constant inflow transport of 30 Sv (1 Sv $\equiv 10^6$ m^3 s^{-1}) is prescribed and is distributed according to measurements from the Subtropical Atlantic Climate Studies (STACS; Leaman et al. 1987). On the eastern boundary, the total of 100 Sv is allowed to exit the domain between 37° and 40°N, while 40 and 30 Sv total inflow enter north of the Gulf Stream, along the continental slope, and south of the Gulf Stream, respectively. These inflows, based on a

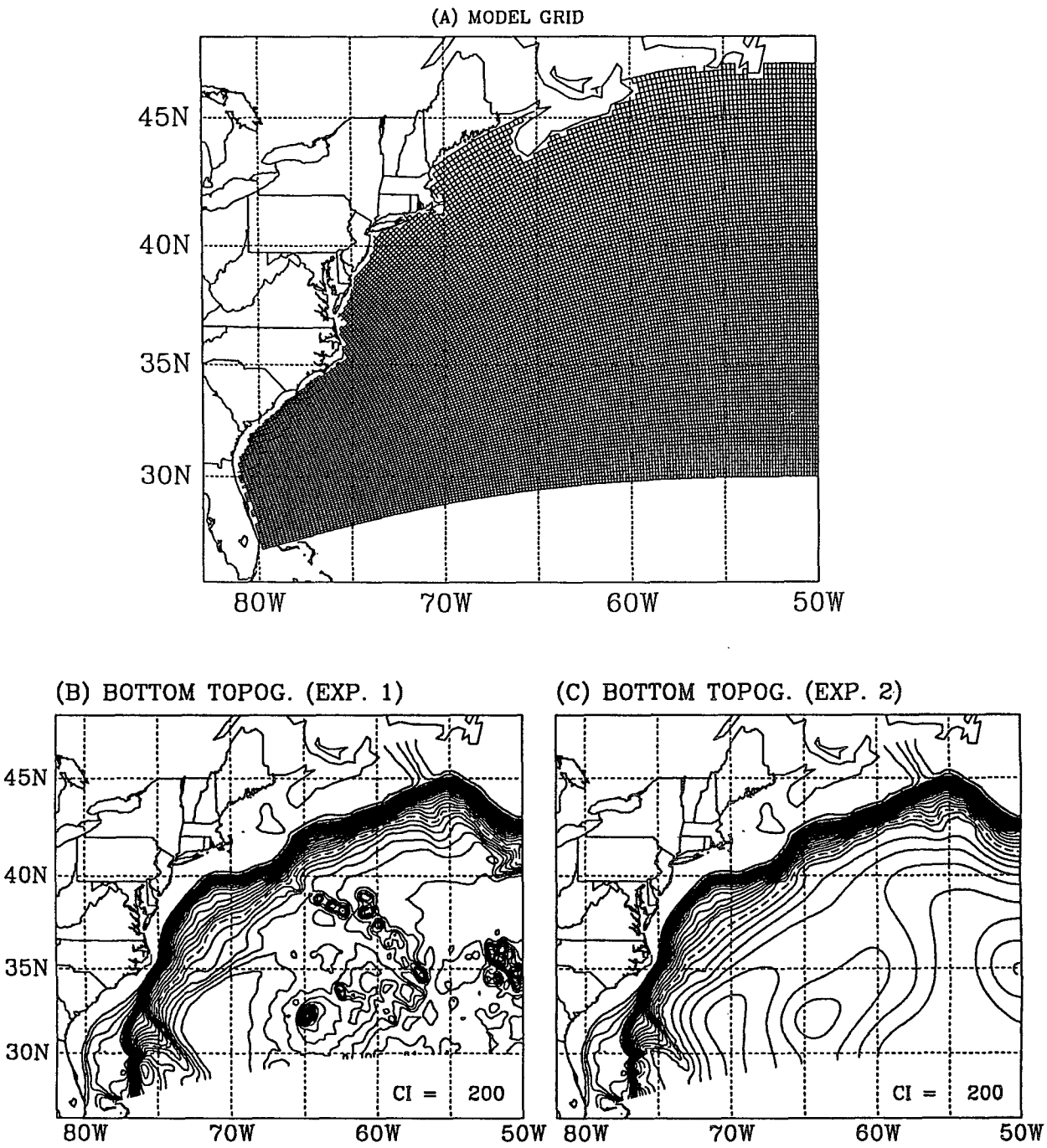

FIG. 1. (a) The curvilinear orthogonal model grid. (b) The bottom topography in experiment 1 (full bottom topography). (c) The bottom topography in experiment 2 (the seamounts are eliminated). The contour interval in (b) and (c) is 200 m; bottom topography in (b) and (c) are identical for regions shallower than 4000 m (the dashed contour).

diagnostic calculation (Mellor et al. 1982) and observations (Richardson 1985; Hogg et al. 1986), represent the northern recirculation gyre and the subtropical gyre. Except for the Florida Straits, the rest of the open boundaries are governed by the Sommerfeld radiation condition. Therefore, although the total transport on the open boundaries is prescribed, the internal velocities are free to adjust to the density field. Temperature and salinity on the open boundaries are prescribed from the observed climatologies, and are advected into the model domain when flow is into the model domain.

The surface boundary conditions include heat flux and wind stress obtained from a 2° × 2° monthly averaged climatology of the Comprehensive Ocean–Atmosphere Data Set (COADS) analyzed by Oberhuber (1988), together with a one-way model feedback scheme. They are described in detail by Ezer and Mellor (1992). Surface salinity fluxes are zero here; however, preliminary analysis of experiments in which surface salinity fluxes and river runoff are added indicate that these fluxes may be important for the coastal ocean, but have only a small effect on the Gulf Stream.

3. The numerical experiments

The model is initialized with the synoptic analysis temperature and salinity fields of 4 May 1988 obtained from the Optimum Thermal Interpolation System (OTIS), developed at the U.S. Navy's Fleet Numerical Oceanography Center; the global ocean OTIS is described by Clancy et al. (1990), and the regional OTIS used here is described by Cummings and Ignaszewski (1991). In the western North Atlantic, it uses satellite sea surface temperature images, as well as other observations and a feature model to construct the Gulf Stream and its associated rings; the data were provided by the Institute for Naval Oceanography. More details about the OTIS analysis and how it is used to initialize the model can be found also in Ezer et al. (1992, 1993), who used this data for nowcast and forecast experiments.

The initialization approach consists of 10 days of a diagnostic calculation (holding T and S constant) to produce nearly geostrophic velocities and surface elevation, and then an additional 30 days of a prognostic calculation (during this time the model develops its own meanders and rings). In this paper we discuss the analysis of a one-year simulation that followed the initialization described above. It should be noted here that initialization of a large-scale ocean model with density field $\rho = \rho(z)$ or with a coarse-resolution climatological data $\rho = \rho(x, y, z)$ requires much longer spinup time. However, here we use for initialization high-resolution (0.2° × 0.2° horizontal grid and 34 vertical levels) data, including observations taken around the initialization day plus the position of the Gulf Stream's meanders and eddies. Moreover, with the high-resolution regional model, which is largely driven by the imposed flows on the open boundaries, the adjustment time is of the order of the dominant scales of the region (around 20 days), as indicated in previous studies with similar initialization (e.g., Mellor and Ezer 1991; Ezer and Mellor 1992; Ezer et al. 1992). In fact, during the short spinup time, the flow is dynamically balanced enough to demonstrate a considerable forecast skill for at least a two-week period (Ezer et al. 1992). Experiments (not shown) with longer spinup time show the same results as those presented here (e.g., the mean and the variance of, say, the first and the second year of the simulation are very similar). Although interannual variabilities are neglected here, with the expected improvement in computational capabilities, we will focus more attention toward long-term variabilities in future studies.

In this study we present two cases, initialized and forced in the same way but with different bottom topography. In experiment 1 the full bottom topography is included (Fig. 1b), while in experiment 2 the seamounts (mostly the NESC and Bermuda) are removed, leaving the other topographic features such as the continental shelf and slope and the general shape of the bottom of the deep ocean intact (Fig. 1c). We next compare statistics (mean and variability) obtained from a one-year simulation of each experiment. The simulations are also compared with observations.

4. Simulation results

a. The flow fields

The one-year average velocity fields for the case with full bottom topography (experiment 1) and for the case without the seamounts (experiment 2) are shown in Fig. 2. In the upper layers between 55° and 65°W the Gulf Stream is deflected southward just upstream of the NESC and splits into several meanders in experiment 1 (Fig. 2a); this is clearly due to the seamounts since such meandering is absent from experiment 2 (Fig. 2c). Southward deflection of the stream by the NESC is obtained also by other models (Adamec 1988; Hallock et al. 1991) and may be observed in satellite IR images as a quasi-permanent meander (Cornillon 1986); however, it seems that models tend to overreact to this topographic effect, so the observed deflection is usually smaller than that predicted by models. A deflection of a jet flowing over a ridge is expected from the conservation of potential vorticity; however, the response is more complicated here since the topographic features consist of individual seamounts with sizes comparable to the mesoscale features of the Gulf Stream system.

The simulated flow at 1500 m (Figs. 2b,d) shows the eastward flow of the deep Gulf Stream and the westward flow of the deep western boundary current (DWBC) along the continental slope. The latter flow marks the edge of the northern recirculation gyre (Hogg et al. 1986) formed in the model by the nearly barotropic slope water inflow that enters the domain near the northeast boundary; the upper portion of it is entrained into the Gulf Stream around 75°W, while the deep part (i.e., the DWBC) crosses under the Gulf Stream and exits the model domain at the southwest boundary. While experiment 2 shows smooth, weak recirculation flow in the deep ocean (Fig. 2d), experiment 1 shows several strong recirculation gyres north and south of the stream (Fig. 2b). The transport of the DWBC also increases when the seamounts are included in the calculation. Several studies have demonstrated

the important role played by the DWBC in the separation of the Gulf Stream. In the model used by Thompson and Schmitz (1989), the DWBC outflow was imposed as boundary condition on the lower layer of their two-layer model, whereas here and in Ezer and Mellor (1992), who studied the Gulf Stream separation, the DWBC is developed by the model dynamics as the continuation of the slope water inflow imposed on the northern part of the eastern open boundary.

The total streamfunction, Ψ, calculated from the vertically averaged velocity field, is shown for experiments 1 and 2 in Figs. 3a and 3b. While experiment 2 results in a smooth and straight Gulf Stream path, the inclusion of the seamounts in experiment 1 results in increasing total transport and the development of several subrecirculation gyres and quasi-stationary meanders. Due to these gyres, the total transport of the stream may increase locally by as much as 30–50 Sv. The magnitude of these spatial variations of the total Gulf Stream transport is comparable to the seasonal variations of the Gulf Stream transport (Worthington 1976). This could explain some of the discrepancies in different estimates of the transport; such estimates range from ~70 to ~200 Sv (Richardson 1985) and could be attributed to measurements taken at different cross sections with respect to those subgyres. The existence of these quasi-permanent subgyres has been suggested also by some measurements (e.g., Richardson 1981; Teague and Hallock 1990). Recent analysis of Geosat altimeter data by Kelly (1991) suggests that changes of surface variability along the stream may be due to subgyres similar to those obtained here [Fig. 3a is strikingly similar to Fig. 7 in Kelly (1991)].

We now discuss possible mechanisms for the formation of these gyres and for the increase in total transport when the seamounts are included in the calculation. First we discuss a simple case to estimate whether a Taylor column effect (Taylor 1923) may be possible here. In a one-layer nonstratified fluid of depth H flowing over an object of height ΔH and diameter $2R$, the fluid will flow around the object rather than over it if the following condition is satisfied,

$$\frac{\Delta H f R}{H V} > 1, \qquad (1)$$

where f is the Coriolis parameter and V the undisturbed flow speed. For a typical seamount in our case, $\Delta H/H \approx 0.5$, and $V/fR \approx 0.8\ \text{m s}^{-1}/(10^{-4}\ \text{s}^{-1} \times 2 \times 10^4\ \text{m}) = 0.4$. Therefore, (1) is satisfied for those estimated values and it seems possible that the flow will have tendency to meander between individual seamounts rather than flow above them; for stronger velocities as observed in the Gulf Stream or for smaller seamounts as some of them are, considerable flow may still cross the NESC. The above discussion is based, of course, on a very rough estimate and simple assumptions, but it nevertheless indicates that such a mechanism is possible.

In a more realistic case than the one assumed in (1), where $H(x, y)$ and $\rho(x, y, z)$, the interaction between an oceanic flow and the bottom topography, is often described in terms of the joint effect of baroclinicity and bottom relief—the so-called JEBAR effect, first introduced by Sarkisyan and Ivanov (1971). To understand this effect we write the vertically integrated vorticity balance equation,

$$J(\Psi, f/H) = J(\phi, 1/H) + \text{wind term} \qquad (2)$$

(Mellor et al. 1982; Greatbatch et al. 1991), where $J(A, B) = (\partial A/\partial x)(\partial B/\partial y) - (\partial A/\partial y)(\partial B/\partial x)$ is the Jacobian operator. The first term on the right-hand side of (2) is the JEBAR term, that is, the forcing due to the interaction between the stratification represented by ϕ, the potential energy per unit area of the water column, and bottom topography, H. Therefore, the streamfunction, Ψ, is strongly affected by bottom topography gradients, when integrating along planetary potential vorticity (f/H) contours. Indeed, diagnostic models of the North Atlantic Ocean have shown significant enhancement of total transport relative to a flat bottom case, due to the JEBAR effect (Holland and Hirschman 1972; Mellor et al. 1982; Greatbatch et al. 1991). The increase in total transport in experiment 1 compared to experiment 2 may be the result of a similar mechanism; large gradients of bottom topography associated with the steep seamounts and strong stratification in the Gulf Stream do exist here.

b. The variations of surface elevation

The rms of sea surface height (SSH) derived from two years of the Geosat altimeter is shown in Fig. 4 [the interpolation method described by Ezer et al. (1993) was used to interpolate data from satellite tracks onto model grid]; it will be compared with the rms SSH derived from the two model calculations (Figs. 5b,d). Also shown in Figs. 5a,c are the mean SSH of the two cases. First, note that the mean SSH shows, again, the deflection of the stream and the meanders produced by the NESC. There are obvious differences and some similarities between the simulated and the observed variabilities. Model variability near the eastern boundary is somewhat reduced, for example, because of the open boundary condition (e.g., eddies generated east of the model domain and drifted into the region cannot be represented in such a regional model). The maximum rms SSH just downstream of Cape Hatteras at 72°–73°W is seen in the altimetry data as well as in the two model runs. However, while the maximum observed variability upstream of the NESC at ~63°W (Fig. 4) is seen in the simulation with realistic topography (Fig. 5b), it is shifted downstream to about 60°W in the case where the NESC was eliminated (Fig. 5d). The fact that maximum variability is obtained in the middle of the domain even without the seamounts may be due to the larger surface forcing variations there

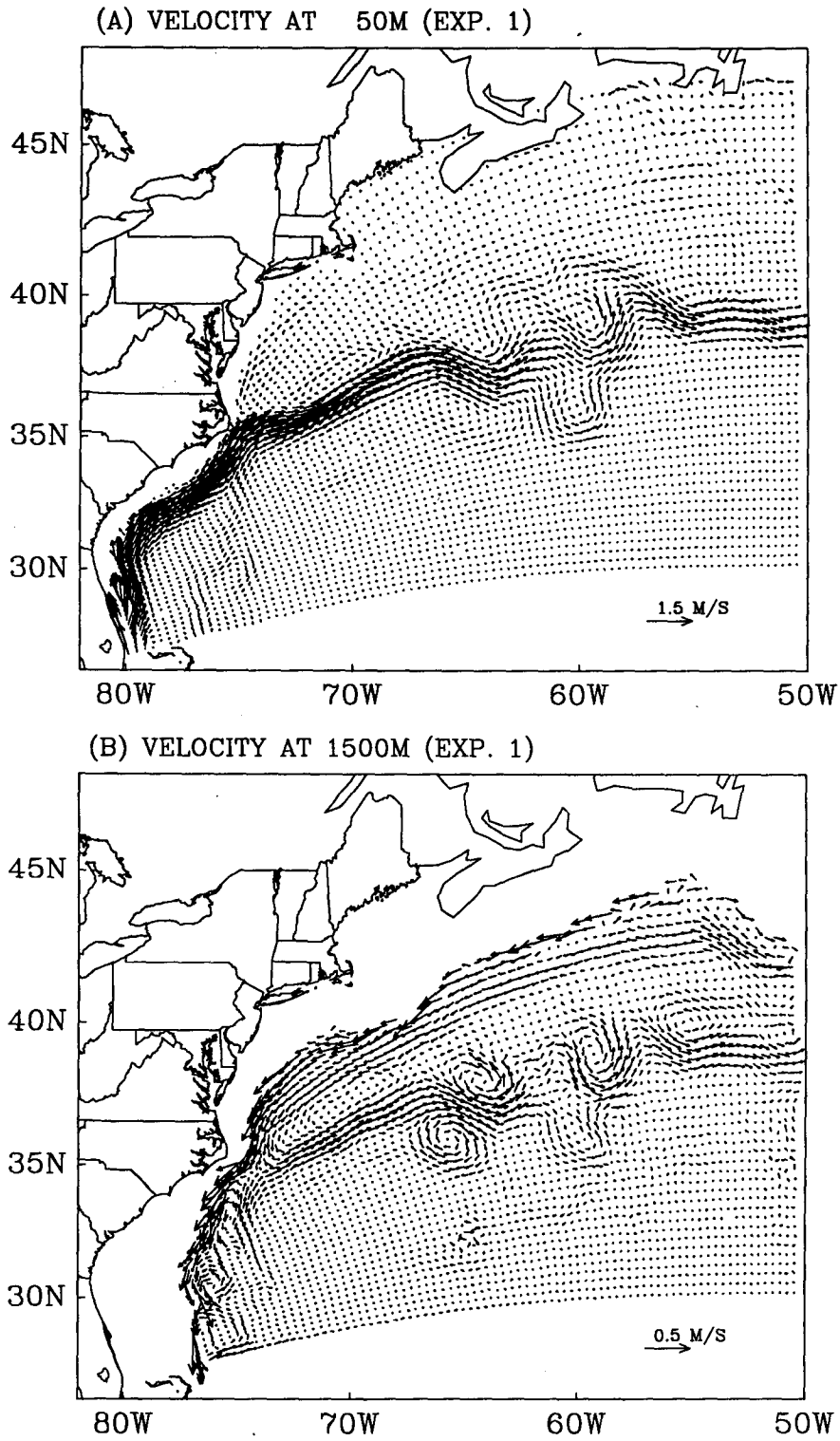

FIG. 2. One-year average velocity vectors: experiment 1 (a) at 50 m and (b) at 1500 m; experiment 2 (c) at 50 m and (d) at 1500 m. A scale vector is indicated at the bottom-right corner of each plot.

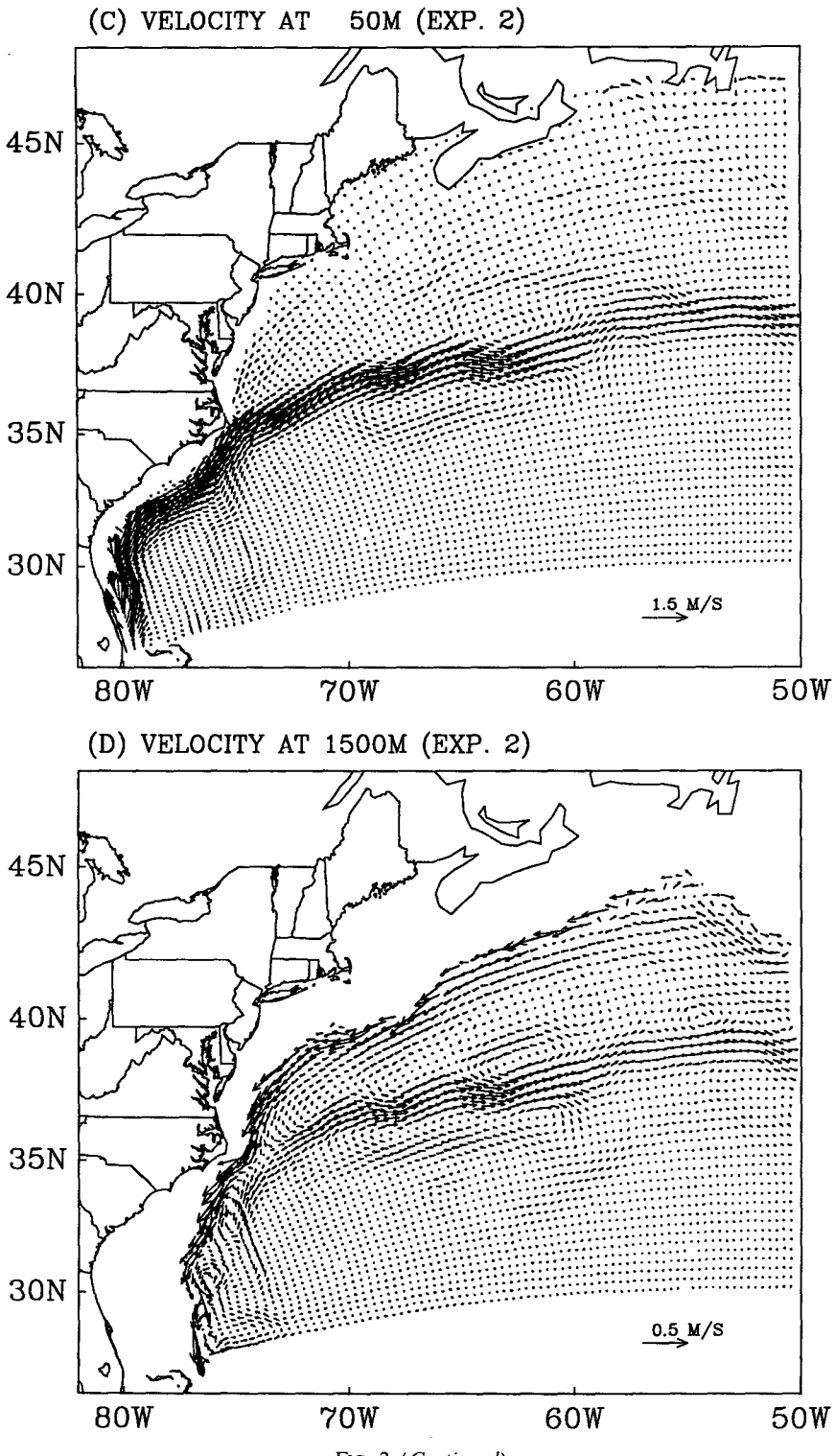

FIG. 2. (*Continued*)

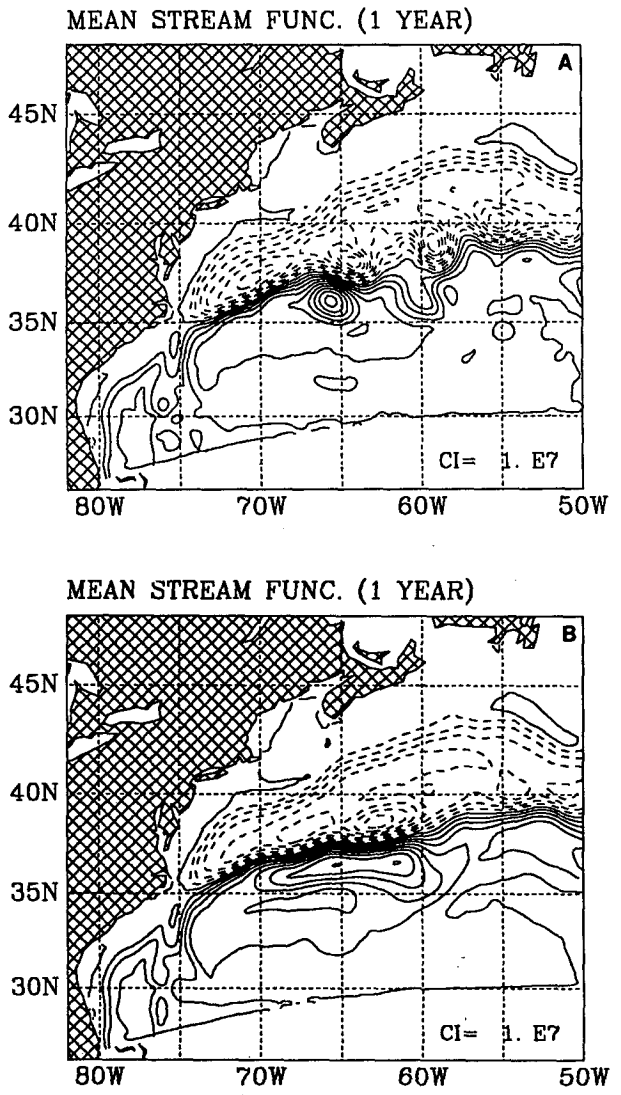

FIG. 3. A one-year mean total streamfunction calculated from the vertically averaged velocity: (a) experiment 1; (b) experiment 2. The contour interval is 10 Sv (10^7 m^3 s^{-1}).

[Ezer and Mellor (1992) show the surface forcing in the area as obtained from Oberhuber (1988)]; however, the main effect of the seamounts is to shift this maximum upstream of the NESC.

c. *The mean and the eddy kinetic energy*

Figure 6 shows the spatial distribution of the eddy kinetic energy (EKE) calculated from the one-year simulation of each case. The differences between the two experiments will be discussed later, but first, we pause for comparison of model results with observations. In general, the EKE obtained from the model calculation with full topography agrees fairly well with observations within a factor of ~2. For example, the surface EKE between 65° to 70°W as inferred from surface drifters analyzed by Richardson (1983) is about 2000 cm^2 s^{-2} with a peak of ~3000 cm^2 s^{-2}, while the model has calculated maximum surface EKE of about 1500 cm^2 s^{-2} with the maximum at similar locations as observed (Fig. 6a). The maximum observed EKE in the deep ocean (H > 4000 m) is ~50–100 cm^2 sec^{-2} in this area (Weatherly 1984; Ezer and Weatherly 1991), compared to ~60 cm^2 s^{-2} in the model simulations. The somewhat underestimated values of simulated EKE is typical of numerical models—for example, Thompson and Schmitz (1989) and Treguier (1992); higher frequency of atmospheric forcing and higher horizontal and vertical model resolution are needed to account for the larger range of the observed oceanic variabilities. In the model discussed here, for example, the upper mixed layer is marginally resolved and the bottom boundary layer is underresolved.

We now look at the differences between the two experiments. The EKE at the upper layers is only slightly affected by the bottom topography, reflecting the shift in the position of the stream (Figs. 6a,c), but larger effects occur in the deeper layers (Figs. 6b,d). The major effect of the seamounts is to shift the area of maximum EKE upstream (westward) of the NESC, and to decrease the maximum values. A possible mechanism for the fact that maximum variability occurs upstream of the NESC is the existence of southwestward propagating (along isobaths) topographic waves generated by the interaction of the meandering stream with the seamounts; such propagating waves have been observed on the continental rise in the vicinity of the NESC (e.g., Thompson 1977; Hogg 1981). It is interesting to note that a similar effect has been simulated by a nu-

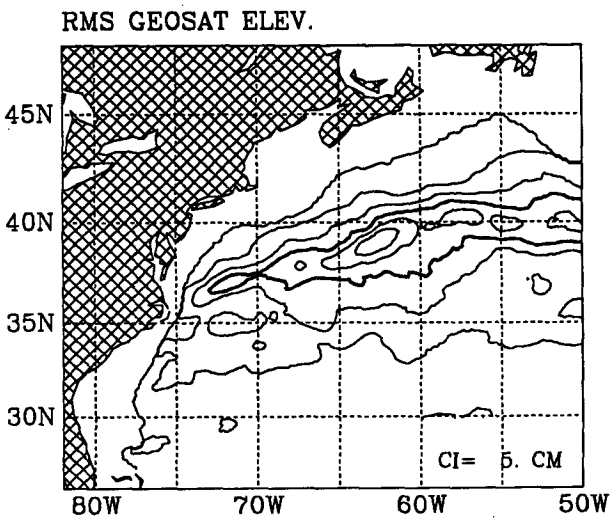

FIG. 4. The rms of sea surface height obtained from two years of Geosat altimeter data (from November 1986 to November 1988). Data were used only for regions where water depth is larger than 1000 m (the 1000-m isobath is the shorewardmost contour). The contour interval is 5 cm; the wider line is the 20-cm contour.

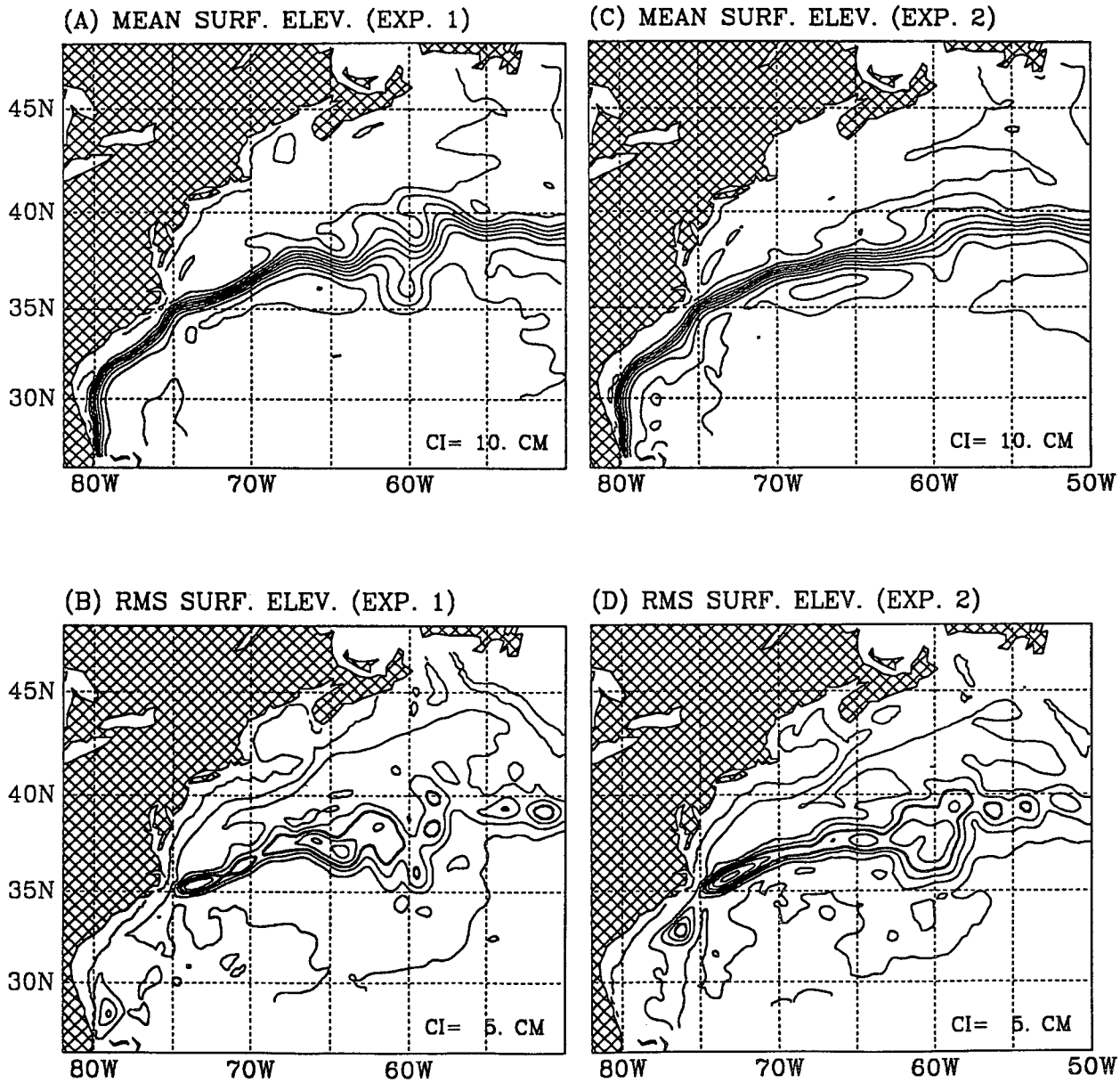

FIG. 5. The (a) mean and (b) rms surface elevation obtained from the one-year run of experiment 1; (c) and (d) are as (a) and (b) but for experiment 2. The contour intervals are 10 and 5 cm for the mean and the rms, respectively; the wider lines in (b) and (d) are the 20-cm contours.

merical model of the South Atlantic Bight, where disturbances upstream of the topographic feature known as the Charleston Bump were attributed to topographic waves generated by the interaction of the Gulf Stream with the bump (Oey et al. 1992). Other contributors to the large variability upstream of the NESC are Gulf Stream eddies. In the model simulations, eddy formation is more frequent near the NESC than in any other region (also observed by Auer 1987); the eddies propagate westward and contribute to the large variability of the western portion of the domain.

To understand the spatial changes associated with the NESC, we now divide the Gulf Stream region into two subregions—the eastern Gulf Stream (north of 35°N, east of 60°W, and where $H > 2000$ m) and the western Gulf Stream (north of 35°N, west of 60°W, and where $H > 2000$ m)—and calculate the area-averaged vertical profiles of EKE and MKE for each subregion; they are shown in Fig. 7. Also shown in Figs. 7c, f are the differences in MKE and EKE between the two experiments; the differences are expressed in % where a positive/negative value means an increase/

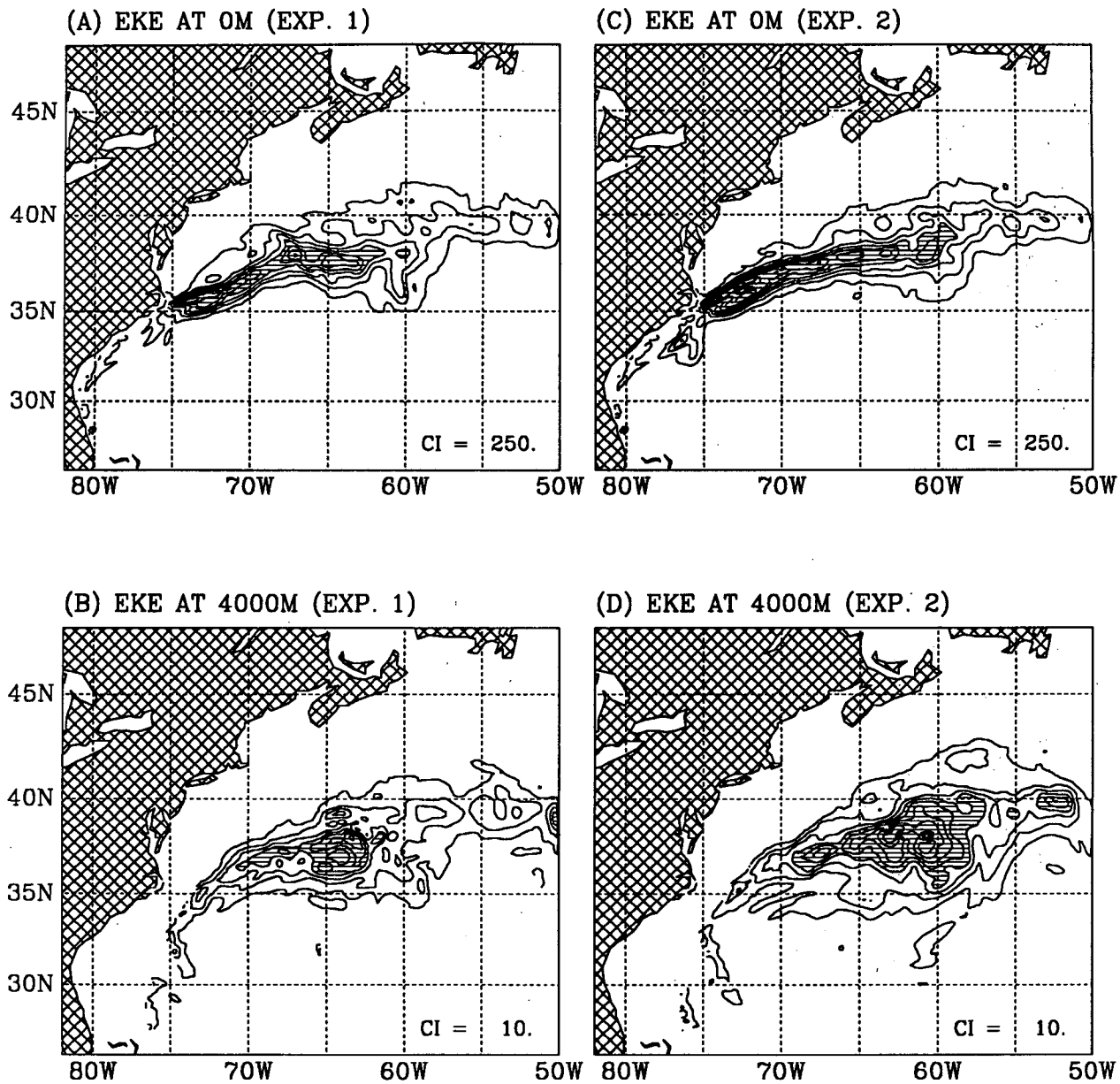

FIG. 6. Eddy kinetic energy (per unit mass): experiment 1 (a) at 0 m and (b) at 4000 m; experiment 2 (c) at 0 m and (d) at 4000 m. The contour intervals are 250 $cm^2 s^{-2}$ for (a) and (c) and 10 $cm^2 s^{-2}$ for (b) and (d). The shaded area represents regions with EKE > 1000 $cm^2 s^{-2}$ for (a) and (c) and EKE > 40 $cm^2 s^{-2}$ for (b) and (d).

decrease in EKE or MKE when the NESC is included in the calculation. As discussed before and indicated in Fig. 6, significant differences are found between the eastern and the western portions of the Gulf Stream. Figure 7 indicates that the area-averaged MKE and EKE are larger by about a factor of 2 in the west region (upstream of the NESC) compared to the east region; this result was obtained in both experiments. (In the vicinity of the Gulf Stream, EKE and MKE have similar orders of magnitude.) West of the NESC, the topographic effect is smaller than east of the seamounts (Figs. 7c, f). In the deep ocean, MKE is always larger, and EKE is always smaller in simulations with the NESC compared to simulations without the NESC. This is the result of the JEBAR effect and the development of the barotropic subgyres described before, which stabilize the flow. The exception is the upper 2500 m of the region upstream of the seamounts where MKE reduces by ~10% in experiment 1; this is probably the result of the blocking effect of the seamounts (a Taylor column effect). Although one expects topographically induced variabilities (e.g., Auer 1987 re-

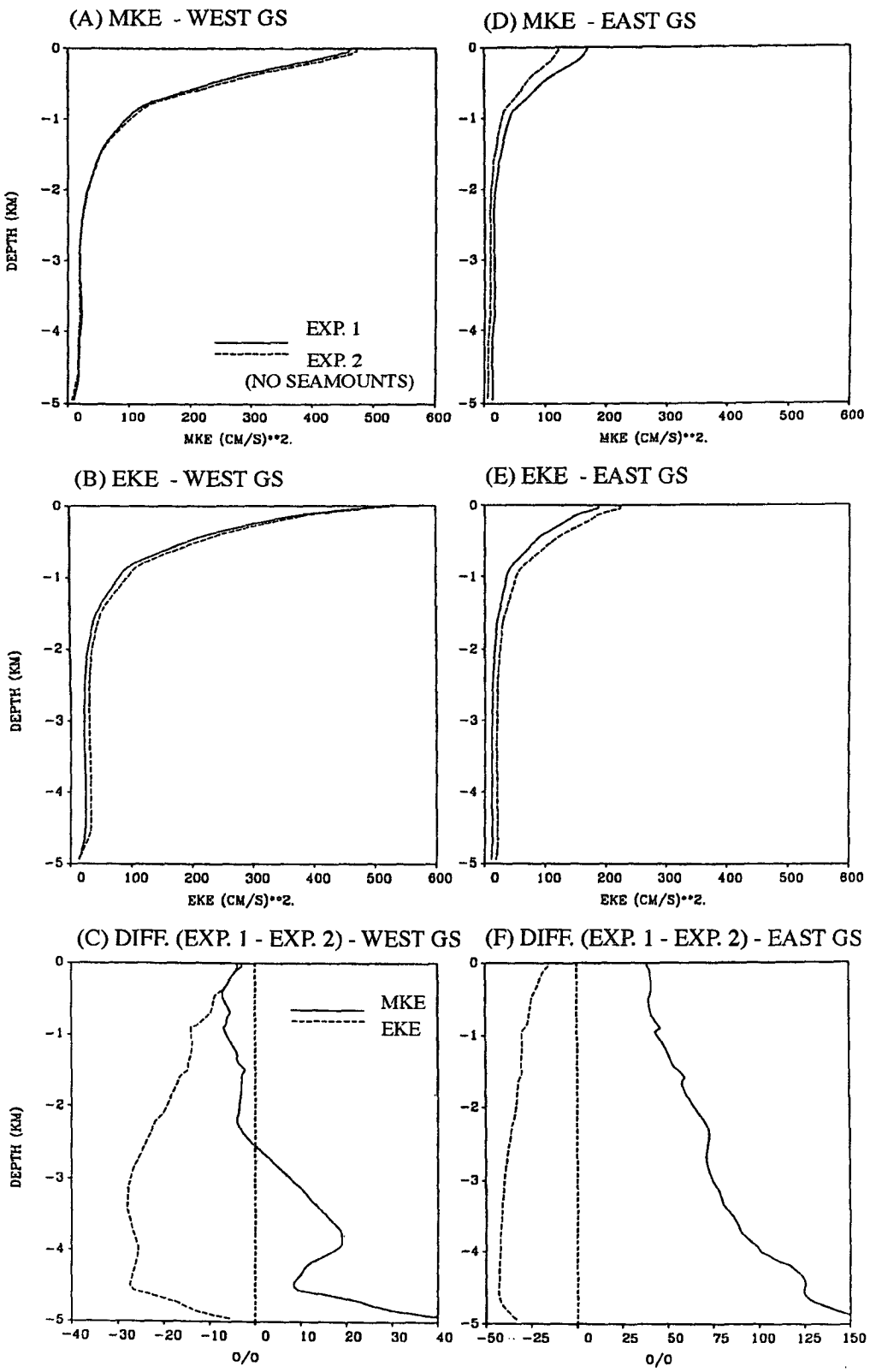

FIG. 7. Area-averaged profiles of (a) MKE in the western Gulf Stream region, (b) EKE in the western Gulf Stream region (solid line, experiment 1; dashed line, experiment 2), (c) difference (in %) between experiment 1 and 2 (solid line, MKE; dashed line, EKE). (d)–(f) are as (a)–(c) but for the eastern Gulf Stream region.

ported that the largest frequency of warm-core ring formation occurs near the NESC), it seems from our experiments that the stabilizing topographic effect dominates.

d. Propagation and growth of Gulf Stream meanders

Analysis of the Gulf Stream path from satellite IR imagery by Cornillon (1986) showed a complicated picture of a meandering stream in the vicinity of the NESC. It also indicated interannual variabilities whereas, for example, a quasi-permanent meander just upstream of the NESC was observed in 1982 and in 1984 but not in 1983. The experiments done here were not, of course, long enough to account for interannual variabilities, but nonetheless, they suggest that such a quasi-permanent meander, obtained also in our simulations at a similar location as observed (Fig. 3a), is topographically induced.

We now compare the Gulf Stream path evolution in the two experiments; the path is obtained from the maximum gradient of sea surface height across the stream and plotted every 5 days in Fig. 8. The evolution of the simulated Gulf Stream compares quite well with the observed evolution. For example, the simulated Stream shows a change from a region of smooth path in the western portion of the domain to a region with increasing meander amplitudes downstream (Fig. 8a), as seen in the observations (Fig. 1 in Cornillon 1986). In both model experiments, steep and convoluted meanders are obtained between 60° to 65°W, which may indicate that this change in the evolution of the stream is not directly related to the NESC. Even without the NESC (i.e., experiment 2), the model calculation shows a larger frequency of eddy formation there, as observed by Auer (1987). Thus, the general shape of the basin topography or external forcing may be responsible for these changes. However, there are differences between the two experiments that could be attributed to the NESC. When the seamounts are neglected, the downstream propagation speed of the Gulf Stream meanders is almost uniform across the domain (Fig. 8b). On the other hand, with full topography, propagation speed changes (usually decreases downstream; Fig. 8a) with abrupt changes similar to those described by Cornillon (1986). (The solid lines in Figs. 8a,b show examples of propagating meanders, where a steeper line corresponds to a slower moving meander.) Downstream of the seamounts, a large, almost stationary meander is obtained here in experiment 1, with small upstream propagation direction (upstream propagation at the same area was also indicated by Cornillon 1986).

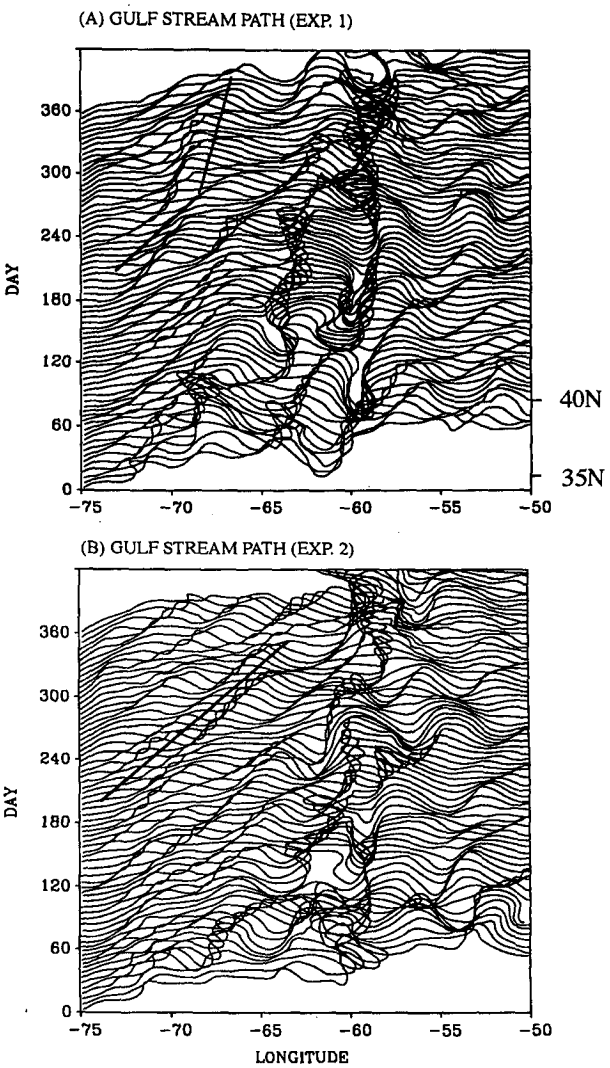

FIG. 8. Gulf Stream path evolution obtained from the maximum sea surface gradients for (a) experiment 1, (b) experiment 2. The paths are plotted in 5-day intervals; the left end of each path corresponds to its time; the north–south scale is indicated for the first path at $t = 0$. The solid lines show examples of propagating meanders.

5. Discussion and conclusions

The aim of this paper was to report on new findings obtained from a realistic high-resolution regional model of the Gulf Stream region. Of special interest are the topographic effects associated with the interaction of the Gulf Stream with the New England Seamount Chain. Previous observations (e.g., Cornillon 1986; Auer 1987; Teague and Hallock 1990) and simpler numerical models (e.g., Adamec 1988; Thompson and Schmitz 1989) have indicated that the NESC may affect the dynamics of the Gulf Stream. However, there is conflicting observational evidence (Cornillon 1986, reviews some of them) and discrepancies between modeled and observed variabilities (e.g., Hallock et al. 1989, 1991). Therefore, by using a more realistic numerical model in this study, we wish to advance our understanding of the interaction between an energetic

jet and complicated mesoscale topographic features such as the seamounts chain.

The approach here was to compare a model simulation with full bottom topography to a control simulation where the NESC is removed. Unlike previous numerical studies of this type where the control run includes a flat bottom case (e.g., Adamec 1988; Thompson and Schmitz 1989), here, other topographic features such as the continental shelf and slope and the general topography of the basin remain unchanged. Therefore, effects associated directly with the NESC are isolated from other topographic effects. The rms sea surface height and EKE in the model with full topography are quite realistic and compared favorably with previous observations. The main spatial effect of the NESC is to shift the area of maximum variability (as inferred from rms surface elevation and EKE) upstream of the NESC. It is suggested that the upstream maximum in deep ocean variability may be due to topographic waves propagating westward (as observed in this area by Thompson 1977 and Hogg 1981), generated by the interaction of the Gulf Stream with the NESC. Furthermore, in the region near the NESC, eddies are formed more frequently than in other regions (Auer 1987); these eddies propagate westward and contribute to the large variability of the upper ocean in the western portion of the Gulf Stream region. The eddy-induced variations upstream of the NESC may also induce variations in the deep ocean. For example, Ezer and Weatherly (1991) have analyzed observations that show that the MKE and the EKE of the near-bottom layers are highly correlated with the variations of the upper layers in the vicinity of the Gulf Stream, on time scales ranging from several days to seasonal scales; correlation was especially high in the eddy time-scale range (about 90 days).

The topographic effect seems to stabilize the flow and to generate several quasi-stationary meanders and subgyres. These gyres have a large barotropic component, and their spatial scale is ~400 km—larger than mesoscale eddies but smaller than the northern and southern recirculation gyres of the Gulf Stream. Previous observations have suggested the existence for such gyres (e.g., Richardson 1981; Teague and Hallock 1990); however, it has been demonstrated here that they are topographically induced by the interaction of the strong Gulf Stream flow with the NESC. The transport associated with these subrecirculation gyres is ~30–50 Sv, comparable to the seasonal changes of the Gulf Stream transport reported by Worthington (1976). Although the NESC may enhance meandering and eddy formation, the stabilizing effect of the seamounts dominates and EKE is reduced for the entire water column when the NESC is included in the calculations. The study also suggests that the NESC causes a downstream decrease in the propagation speed of Gulf Stream meanders.

This study describes preliminary results obtained from a more realistic Gulf Stream model than previous studies; more in-depth analysis and more comparisons with observations will be provided in the future. Further improvements in the horizontal and the vertical resolution of the model are clearly needed (the vertical grid has smaller grid size near the surface and larger near the bottom, thus the surface mixed layer is resolved, but the bottom boundary layer is not). Ezer and Weatherly (1990, 1991), for example, showed that bottom boundary-layer dynamics play an important role in this region. In any case, the study demonstrates the importance of resolving mesoscale topographic features as well as mesoscale oceanic features in numerical models. Therefore, it calls for further theoretical and numerical studies of the small-scale ocean circulation–topography interaction.

Acknowledgments. Thanks are due to G. L. Mellor for much help and advice during the study. The reviewers and the editor had very helpful suggestions. The support of the Office of Naval Research (Contract N00014-93-1-10037), the Institute for Naval Oceanography, the National Ocean Service, and NOAA's Geophysical Fluid Dynamics Laboratory are gratefully acknowledged.

REFERENCES

Adamec, D., 1988: Numerical simulations of the effects of seamounts and vertical resolution on strong ocean flows. *J. Phys. Oceanogr.*, **18,** 258–269.

Auer, S. J., 1987: Five-year climatological survey of the Gulf Stream system and its associated rings. *J. Geophys. Res.*, **92,** 11 709–11 726.

Blumberg, A. F., and G. L. Mellor, 1987: A description of a three-dimensional coastal ocean circulation model. *Three-Dimensional Coastal Ocean Models,* Vol. 4, N. Heaps, Ed., Amer. Geophys. Union, 208 pp.

Bryan, F., and W. R. Holland, 1989: A high-resolution simulation of the wind and thermohaline-driven circulation of the North Atlantic Ocean. *Proc. Hawaiian Winter Workshop, 'Aha Huliko'a,* University of Hawaii, 99–116.

Clancy, R. M., P. A. Phoebus, and K. D. Pollak, 1990: An operational global-scale ocean thermal analysis system. *J. Atmos. Oceanic Technol.*, **7,** 233–254.

Cornillon, P., 1986: The effect of the New England Seamounts on Gulf Stream meandering as observed from satellite IR imagery. *J. Phys. Oceanogr.*, **16,** 386–389.

Cummings, J. A., and M. J. Ignaszewski, 1991: The Fleet Numerical Oceanography Center regional ocean analysis system. MTS '91, *Proc. Marine Technology Society,* New Orleans, 1123–1129.

Ezer, T., and G. L. Weatherly, 1990: A numerical study of the interaction between a deep cold jet and the bottom boundary layer of the ocean. *J. Phys. Oceanogr.*, **20,** 801–816.

——, and ——, 1991: Small-scale spatial structure and long-term variability of near bottom layers in the HEBBLE area. *Deep Ocean Sediment Transport. Mar. Geol.*, **99,** 319–328.

——, and G. L. Mellor, 1992: A numerical study of the variability and the separation of the Gulf Stream induced by surface atmospheric forcing and lateral boundary flows. *J. Phys. Oceanogr.*, **22,** 660–682.

——, D.-S. Ko, and G. L. Mellor, 1992: Modeling and forecasting the Gulf Stream. *Oceanic and Atmospheric Nowcasting and*

Forecasting, D. L. Durham and J. K. Lewis, Eds., *Mar. Technol. Soc. J.,* **26**(2), 5–14.

——, G. L. Mellor, D.-S. Ko, and Z. Sirkes, 1993: A comparison of Gulf Stream sea surface height fields derived from Geosat altimeter data and those derived from sea surface temperature data. *J. Atmos. Oceanic Technol.,* **10,** 76–87.

Greatbatch, R. J., A. F. Fanning, A. D. Goulding, and S. Levitus, 1991: A diagnosis of interpentadal circulation changes in the North Atlantic. *J. Geophys. Res.,* **96,** 22 009–22 023.

Hallock, Z. R., J. L. Mitchell, and J. D. Thompson, 1989: Sea surface topographic variability near the New England Seamounts: An intercomparison among in situ observations, numerical simulations, and Geosat altimetry from the Regional Energetics Experiment. *J. Geophys. Res.,* **94,** 8021–8028.

——, W. J. Teague, and J. D. Thompson, 1991: A comparison of observed and modeled sea surface topographic time series near the New England Seamounts. *J. Geophys. Res.,* **96,** 12 635–12 644.

Hogg, N. G., 1981: Topographic waves along 70°W on the continental rise. *J. Mar. Res.,* **39,** 627–649.

——, R. S. Pickart, R. M. Hendry, and W. J. Smethie, 1986: The northern recirculation gyre of the Gulf Stream. *Deep-Sea Res.,* **33,** 1139–1165.

Holland, W. R., and A. Hirschman, 1972: A numerical calculation of the circulation in the North Atlantic Ocean. *J. Phys. Oceanogr.,* **2,** 336–354.

Kelly, K. A., 1991: The meandering Gulf Stream as seen by the Geosat altimeter: Surface transport, position, and velocity variance from 73° to 46°W. *J. Geophys. Res.,* **96,** 16 721–16 738.

Leaman, K. D., R. L. Molinari, and P. S. Vertes, 1987: Structure and variability of the Florida Current at 27°N: April 1982–July 1984. *J. Phys. Oceanogr.,* **17,** 565–583.

Mellor, G. L., and T. Yamada, 1982: Development of a turbulence closure model for geophysical fluid problems. *Rev. Geophys. Space Phys.,* **20,** 851–875.

——, and T. Ezer, 1991: A Gulf Stream model and an altimetry assimilation scheme. *J. Geophys. Res.,* **96,** 8779–8795.

——, C. Mechoso, and E. Keto, 1982: A diagnostic calculation of the general circulation of the Atlantic Ocean. *Deep-Sea Res.,* **29,** 1171–1192.

Oberhuber, J. M., 1988: An atlas based on the COADS data set: The budgets of heat, buoyancy and turbulent kinetic energy at the surface of the global ocean. Max-Planck-Institut für Meteorologie, Rep. No. 15.

Oey, L-Y., T. Ezer, G. L. Mellor, and P. Chen, 1992: A model study of 'bump' induced western boundary current variabilities. *J. Mar. Sys.,* **3,** 321–342.

Richardson, P. L., 1981: Gulf Stream trajectories measured with free drifting buoys. *J. Phys. Oceanogr.,* **11,** 999–1010.

——, 1983: Eddy kinetic energy in the North Atlantic from surface drifters. *J. Geophys. Res.,* **88,** 4355–4367.

——, 1985: Average velocity and transport of the Gulf Stream near 55°W. *J. Mar. Res.,* **43,** 83–111.

Sarkisyan, A. S., and V. F. Ivanov, 1971: Joint effect of baroclinicity and bottom relief as an important factor in the dynamics of sea currents. *Izv. Acad. Sci. USSR, Atmos. Oceanic Phys.,* **7,** 173–188. [English Translation.]

Taylor, G. I., 1923: Experiments on the motion of solid bodies in rotation liquid. *Proc. Roy. Soc. London,* **104,** 213–219.

Teague, W. J., and Z. R. Hallock, 1990: Gulf Stream path analysis near the New England Seamounts. *J. Geophys. Res.,* **95,** 1647–1662.

Thompson, J. D., and W. J. Schmitz, 1989: A limited-area model of the Gulf Stream: Design, initial experiments, and model-data intercomparison. *J. Phys. Oceanogr.,* **19,** 791–814.

Thompson, R., 1977: Observations of Rossby waves near site D. *Progress in Oceanography,* Vol. 7, Pergamon, 1–28.

Treguier, A. M., 1992: Kinetic energy analysis of an eddy resolving, primitive equation model of the North Atlantic. *J. Geophys. Res.,* **97,** 687–701.

Weatherly, G. L., 1984: An estimate of bottom friction dissipation by Gulf Stream fluctuations. *J. Mar. Res.,* **42,** 289–301.

Worthington, L. V., 1976: *On the North Atlantic Circulation.* Johns Hopkins University Press, 110 pp.